

# Poly lactide Films Formed by Immersion Precipitation: Effects of Additives, Nonsolvent, and Temperature

Hassan Sawalha, Karin Schroën, Remko Boom

Food and Bioprocess Engineering Group, Wageningen University, Wageningen, The Netherlands

Received 29 August 2006; accepted 7 November 2006

DOI 10.1002/app.25808

Published online in Wiley InterScience (www.interscience.wiley.com).

**ABSTRACT:** The influence of nonsolvent, crystallinity of the polymer film, and addition of dodecane (a poor solvent for the polymer and for the nonsolvent) on the morphology of polylactides films has been investigated and was related to phase separation behavior. Both amorphous poly-DL-lactide (PDLLA) and crystalline poly-L-lactide (PLLA) were dissolved in dichloromethane, and subsequently films were made by immersion in nonsolvent baths. PDLLA gave dense films without any internal structure, since the structure was not solidified by crystallization or glassification. PLLA films show varying structure depending on the nonsolvent. With methanol, asymmetric morphologies were observed as a result from combined liquid-liquid demixing and crystallization, while with water symmetric spherulitic structures were formed. As a next step, dode-

cane was added, which is not miscible with the nonsolvent, and we found it to have a strong influence on the morphology of the films. The PDLLA films with dodecane did not collapse: a closed cell structure was obtained. In PLLA films, dodecane speeds up phase separation and induces faster crystallization in the films, and the porosity, size of the pores, and interconnectivity increased. When the PLLA solutions were subjected to a heat pretreatment, crystallization could be postponed, which yielded a cellular structure around dodecane, which did not contain spherulites anymore. © 2007 Wiley Periodicals, Inc. *J Appl Polym Sci* 104: 959–971, 2007

**Key words:** polylactide; immiscible additives; morphology; phase separation; (quaternary) phase diagram

## INTRODUCTION

Phase separation of polymer solutions is one of the most popular techniques used, for e.g., the preparation of porous polymeric membranes or dense or hollow particles. Different methods are known such as thermally induced phase separation, air-casting of a polymer solution, precipitation from the vapor phase, and immersion precipitation.<sup>1,2</sup> All these methods are used to produce commercial membranes. For the production of flat sheet membranes, a solution that consists of polymer and solvent is cast on an inert support and subsequently immersed in a coagulation bath filled with a nonsolvent.<sup>3</sup> For the production of hollow fiber membranes, the support is not required because of the construction of the nozzle that shapes the membrane directly.

Because of the exchange of solvent and nonsolvent, phase separation occurs. Two main types of phase transitions are responsible for this, liquid-liquid demixing and solid-liquid demixing.<sup>4,5</sup> Liquid-liquid demixing in polymer solutions that are relatively con-

centrated (typically >10 wt %), generally takes place by nucleation and growth of the polymer poor phase. Solid-liquid demixing mainly happens in crystalline and semicrystalline polymers, and occurs because of crystallization, gelation, or vitrification.<sup>1,6,7</sup> The resulting morphology is strongly determined by the aforementioned processes. Generally, liquid-liquid demixing produces porous and cellular structures, while crystallization forms interlinked particle-based structures.<sup>8–10</sup> Many parameters such as concentration of the polymeric solution, crystallinity of the polymer, temperature of the casting solution and coagulation bath, type of solvent and nonsolvent, and their mutual diffusivities<sup>5,11–15</sup> influence demixing, and consequently the final morphology. Some investigators have reported that additives in the casting solution can be used to modify the structure obtained. As additives, a second polymer, acids, alcohols, or inorganic salts have been reported. Obviously, the resulting morphology strongly depends on the type of additive and the interactions with the polymer, solvent, and nonsolvent.<sup>13,16–19</sup>

In the study reported here, we chose polylactic acid (PLA), which is a biodegradable polymer that has wide applications in the medical and pharmaceutical fields.<sup>20,21</sup> PLA films were formed by means of immersion precipitation, which has, for instance, not only been proposed as a method for the preparation of biodegradable scaffolds for blood vessels, but also for

Correspondence to: H. Sawalha (hassan.sawalha@wur.nl).

Contract grant sponsor: BURST; contract grant number: IS042035.

Contract grant sponsor: SENTER.

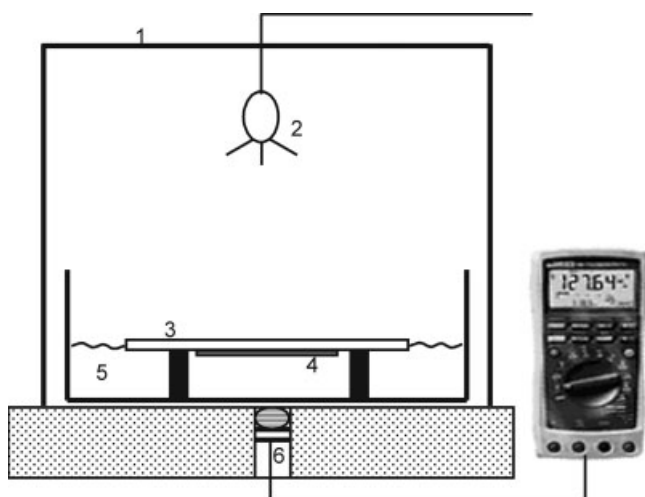


**Figure 1** Experimental setup for light transmission measurement: 1, plastic cover; 2, light source; 3, glass plate; 4, polymer film; 5, coagulation bath; 6, photocell.

preparation of drug delivery devices.<sup>18</sup> Two types of PLA were used: poly(D50,L50)lactide PDLLA and (P(L)LA) PLLA. PDLLA is a random copolymer that cannot crystallize and thus is either in the rubbery or in the glassy state, while PLLA is in optically pure form and crystallizes readily.<sup>11,22,23</sup>

The effects of nonsolvent quality and PLA crystallinity on the resulting film morphology were studied separately. Unlike in most studies, in which additives are used, which are soluble in the nonsolvent,<sup>9,12,18</sup> we have used dodecane as an additive, which is not soluble in the nonsolvent. The effect on the resulting structures is unknown, but it is to be expected that different morphologies can be obtained. The morphology of the films was investigated visually with scanning electron microscopy. Light transmission experiments were performed to monitor and characterize the film formation process itself.

## EXPERIMENTAL

### Materials

Poly-L-lactide (PLLA) and poly-DL-lactide (PDLLA), with an intrinsic viscosity of 1.21 and 0.49 dL/g respectively, were supplied by PURAC Biochem B.V., Gorinchem, the Netherlands. Dichloromethane (DCM) (HPLC, gradient grade) was obtained from Merck (Amsterdam, The Netherlands) and used as the solvent for the polymer. Dodecane ( $\geq 99\%$ ) was purchased from Sigma-Aldrich (Zwijndrecht, The Netherlands) and added to the casting solution as a poor solvent for the polymer. Methanol (HPLC, gradient grade,  $\geq 99.9\%$ ) (Aldrich) was used with Milli-Q water as a nonsolvent. All chemicals were used as received.

### Film preparation

The casting solutions were prepared by dissolving different amounts of polymer in various DCM–dodecane mixtures to obtain the desired concentrations. The solution was kept at the required temperature under stirring for 1–2 days and then cooled down to room temperature before use. Solutions with concentrations (w/w/w) of 20 : 0 : 80, 20 : 5 : 75, 20 : 10 : 70, 20 : 0 : 80 PLLA–dodecane–DCM, and 20 : 10 : 70 PDLLA–dodecane–DCM were used. The polymer solution was cast in the form of a thin film on a glass plate, and subsequently immersed in the coagulation bath for 30 min, after which the films were ready. All the experiments were done at room temperature. As nonsolvents, the following methanol–water mixtures were used: 100 : 0, 60 : 40, 30 : 70, and 0 : 100.

### Light transmission experiments

The experimental setup for light transmission measurements is shown in Figure 1.<sup>3</sup> As mentioned before, the film is cast on a glass plate. The plate is turned upside down, and placed on top of the coagulation bath as quickly as possible. A desk lamp is used as light source just above the coagulation bath. The setup was shielded from ambient light by an opaque plastic cover. The electric resistance was measured by a photocell fixed beneath the coagulation bath. The occurrence of inhomogeneities in the film due to demixing causes the electric resistance to increase; this increase is registered as a function of time.

The curves of resistance in time (an example is shown in Fig. 2) are characterized with three parameters. The first one is the time at which the electric resistance starts to increase, which is considered the onset of demixing (delay time;  $t_d$ ). The time, at which

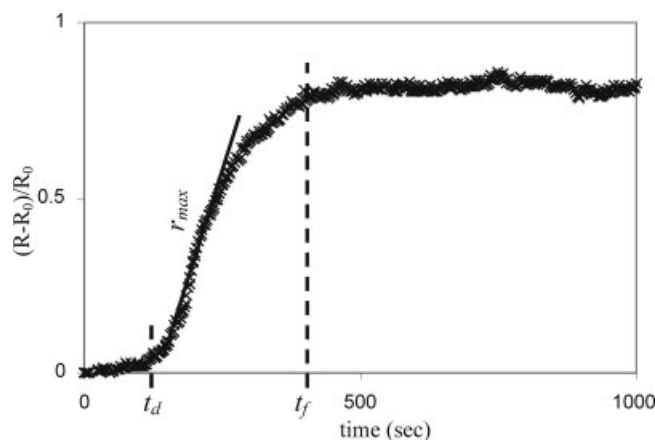


**Figure 2** Interpretation of light transmission results;  $R$  is the electric resistance ( $\Omega$ ) at time  $t$ ,  $R_0$  the initial resistance ( $\Omega$ ),  $t_d$  the delay time of demixing (s),  $r_{max}$  the maximum demixing rate ( $1\text{ s}^{-1}$ ), and  $t_f$  is the time where demixing is complete (s). The actual data were measured for a film of 20 : 10 : 70 PLLA : dodecane : DCM immersed in a water bath.

**TABLE I**  
**Values of the Input Parameters Used in the Equations**

Parameter	Value	Parameter	Value
$\chi_{12}$ (methanol-DCM)	0.5 <sup>19</sup>	$v_1$ (methanol)	40.46 cm <sup>3</sup> /mol
$\chi_{12}$ (water-DCM)	3.3	$v_1$ (water)	10.00 cm <sup>3</sup> /mol
$\chi_{13}$ (methanol-PLA)	1.5 <sup>19</sup>	$v_2$ (DCM)	64.10 cm <sup>3</sup> /mol
$\chi_{13}$ (water-PLA)	3.4 <sup>19</sup>	$v_4$ (dodecane)	226.67 cm <sup>3</sup> /mol
$\chi_{14}$ (methanol-dodecane)	2.5	$r^a$ ( $v_{\text{nonsolvent}}/v_{\text{PLA}}$ )	0.00085 <sup>19</sup>
$\chi_{14}$ (water-dodecane)	3.4	$\Delta H_{m\text{PLA}}$	81–140 J/g <sup>19</sup>
$\chi_{23}$ (DCM-PLA)	0.2 <sup>19</sup>	$T_{m\text{PLA}}^0$	480 K <sup>19</sup>
$\chi_{24}$ (DCM-dodecane)	0.5	$T$	298 K
$\chi_{34}$ (PLA-dodecane)	1.5		

<sup>a</sup> The value of  $r$  is based on the number average degree of polymerization of PLLA with respect to the molar volume of water. This value has to be calculated for each polymer-nonsolvent combination; but because these values have negligible influence in the location of the phase boundaries,  $r$  was taken as a constant value.<sup>19</sup>

the resistance reaches a constant value, represents the final stage of phase separation in the film ( $t_f$ ). In between  $t_d$  and  $t_f$ , the maximum rate of demixing can be found ( $r_{\text{max}}$ ). The curves are analyzed by fitting the logistic growth model, and minimizing the residual sum of squares.

### Scanning electron microscope

The morphology of polymer films was investigated with SEM (JEOL, JSM-5600 LV) (Tokyo, Japan). To prepare cross section samples, sections of the films were cut, dried, and fractured in liquid nitrogen. The top and bottom surfaces and the cross sections were coated with a very thin platinum layer using a sputter-coater (JEOL, JFC-1300) before viewing with SEM.

## METHOD—CALCULATION OF PHASE DIAGRAMS

As many others, we have used the Flory–Huggins theory for evaluating the thermodynamics of the (quaternary) systems used.<sup>1,3,4,6,10,11</sup> The Gibbs energy of mixing is described by

$$\frac{\Delta G_m}{RT} = n_1 \ln \phi_1 + n_2 \ln \phi_2 + n_3 \ln \phi_3 + n_4 \ln \phi_4 \\ + \chi_{12} n_1 \phi_2 + \chi_{13} n_1 \phi_3 + \chi_{14} n_1 \phi_4 + \chi_{23} n_2 \phi_3 \\ + \chi_{24} n_2 \phi_4 + \chi_{34} n_3 \phi_4$$

in which,  $n_i$  is the number of moles of component  $i$ , and  $\phi_i$  is the volume fraction of component  $i$ , and  $\chi_{ij}$  is the Flory–Huggins interaction parameter (see Table I). Index 1 represents the nonsolvent, 2 = solvent, 3 = polymer, and 4 = additive. Because of the complexity of such quaternary systems, we used constant interaction parameters. The main aim of the phase dia-

grams is to show the various trends that are present and not to quantitatively describe all the effects in detail.

The chemical potentials for each component were determined by taking the derivative of the Gibbs energy to  $n_i$ . Phase equilibria were calculated by equating the chemical potential of each component in each phase. This results for a two-phase equilibrium in  $m - 1$  equations ( $m$  is the number of components present), and for a three-phase equilibrium in  $2m - 2$  equations. Solving these equations yields the coexisting compositions, and therewith the binodals. The phase diagrams were shown as limiting ternary phase diagrams, linked together to form the sides of a folded-out pyramidal quaternary phase diagram. For the limiting ternary phase diagram, the volume fraction of the excluded component was set to zero. The ternary phase diagrams (without dodecane) are primarily used in the Results section. The interested reader can find the quaternary phase diagrams in the Appendix, together with a more elaborate explanation for the phase behavior.

The crystallization equilibria were described with the Flory equation for quaternary systems:

$$\frac{v_u \Delta H_m}{v_1 R} \left( \frac{1}{T_m^0} - \frac{1}{T} \right) = \frac{v_1}{v_3} \ln \phi_1 + \frac{v_1}{v_3} (1 - \phi_3) - \phi_1 \\ - \frac{v_1}{v_2} \phi_2 - \frac{v_1}{v_4} \phi_4 + \left( \chi_{13} \phi_1 + \frac{v_1}{v_2} \chi_{23} \phi_2 + \frac{v_1}{v_4} \chi_{34} \phi_4 \right) \\ - \chi_{12} \phi_1 \phi_2 - \chi_{14} \phi_1 \phi_4 - \chi_{24} \phi_2 \phi_4$$

in which  $v_3$  is the molar volume of the repeating unit of Component 3 (PLA), and  $v_i$  the molar volume of component  $i$ ;  $\Delta H_m$  is the melting enthalpy, and  $T_m^0$  the melting temperature of pure PLA. Once more, for the limiting ternary phase diagrams, the volume fraction of the excluded component was set to zero. Values of the parameters used are summarized in Table I.

## RESULTS AND DISCUSSION

### PDLLA films: Nonsolvent effects

To investigate the effect of the type of nonsolvent on the morphology of PDLLA films, a casting solution of 20% w/w PDLLA/DCM was immersed in 100% methanol, 60% w/w methanol/water, and water. The cross sections of all films were similar and consisted of a solid, dense film with no pores; the results for the extremes methanol and water are shown in Figure 3.

When water is used as nonsolvent, the DCM is expected to slowly diffuse through the water phase and evaporate at the surface of the bath. As the miscibility of water with DCM and PLA is very low, one expects that water will hardly penetrate the casting solution. PDLLA is atactic, and therefore amorphous; its

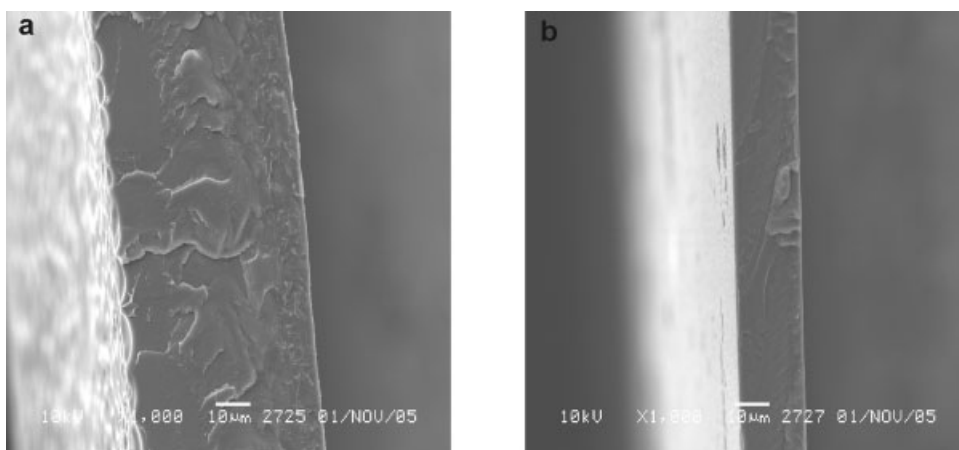


**Figure 3** SEM images of cross sections of films prepared from 20 : 80 w/w PDLLA : DCM with different nonsolvents: (a) methanol, (b) water; please note that the water film has been made out of film with less initial thickness than the one with methanol.

glass transition temperature is expected to be lower than 20°C when it is at equilibrium with water. Therefore, when a PDLLA/DCM film is immersed in a water bath, and the DCM is slowly removed from the film, the PDLLA will not crystallize and the structure will slowly collapse, until all DCM is removed, and a dense film is obtained (see also Fig. 4 for phase diagram).

DCM is only marginally miscible with water but readily miscible with methanol. With methanol, a PDLLA-DCM solution will exhibit so-called delayed demixing (formation of droplets of a polymer lean phase inside the polymer solution, after some time for indiffusion has elapsed).<sup>4</sup> Therefore, one would expect a film containing at least some closed-cell pores because of the presence of the polymer lean phase. This is not what we observed. We expect that the po-

rous structure may have been formed during the process, but as the ultimately formed film is still highly swollen with methanol (PDLLA swells 22% w/w in methanol), it will never reach the glass transition.<sup>11</sup> Thus, the film will never fixate, and the porous structure that is formed initially will have collapsed into a completely dense film when the residual DCM evaporates.

It is known from literature that fixation of the cellular structure obtained by liquid–liquid demixing requires a solidification step.<sup>11</sup> This can take place via solid–liquid demixing (i.e., crystallization), or via glassification. If neither of these transitions occurs, liquid–liquid demixing will proceed until two completely separated layers are obtained.<sup>11</sup> Since PDLLA cannot crystallize,<sup>11,22</sup> and its glass transition line does not cross the binodal for either methanol or water (this

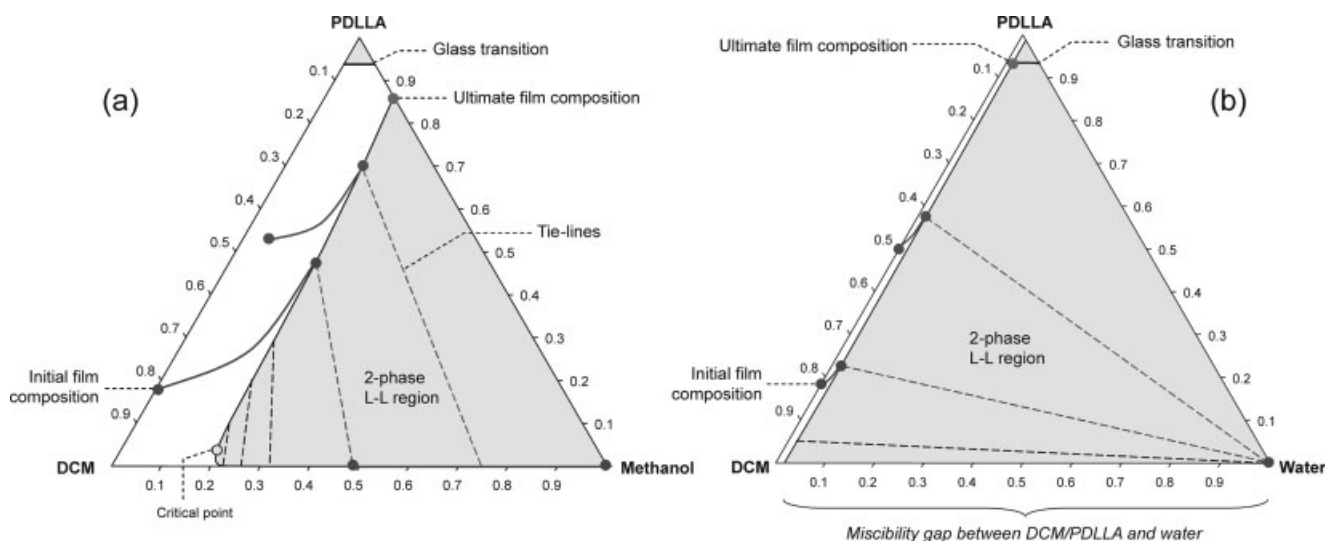


**Figure 4** Schematic equilibrium phase diagram for (a) PDLLA–DCM–methanol and (b) PDLLA–DCM–water. The phase diagrams were calculated with the parameters as mentioned in Table I.

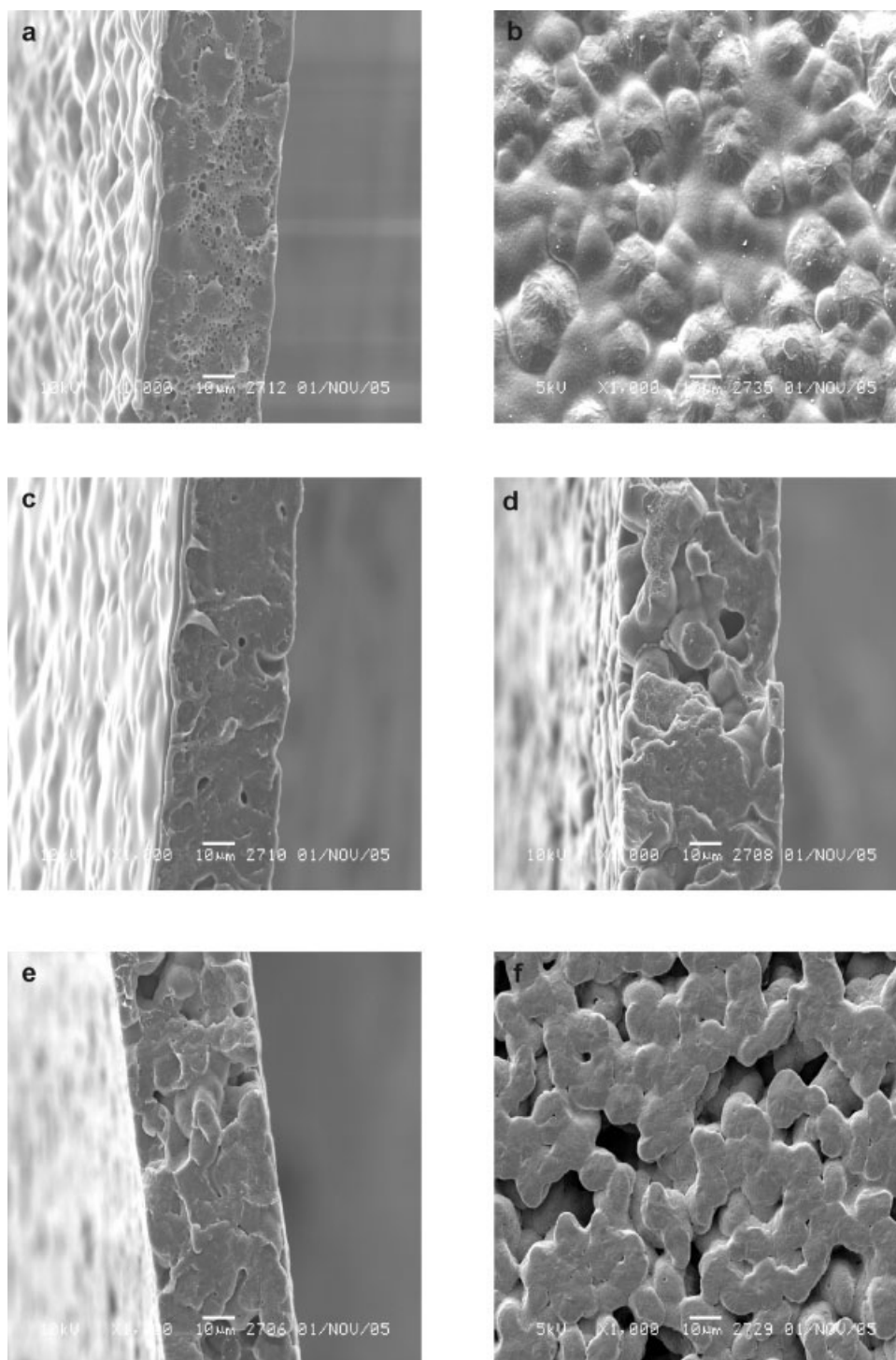


**Figure 5** SEM images of cross sections of films prepared from 20 : 80 w/w PLLA : DCM with different nonsolvents: (a) methanol, (b) methanol, top surface, (c) 60 : 40 w/w methanol : water, (d) 30 : 70 w/w methanol : water, (e) water, (f) water, top surface.

is illustrated in Fig. 4), it will not be solidified but will collapse given sufficient time. Van de Witte et al. have shown with differential scanning calorimetry (DSC) that in a PDLLA–chloroform–methanol system, phase transition occurred only by liquid–liquid demixing and no signs of crystallites or transitions due to verifi-

cation were observed,<sup>24</sup> which is in line with our findings.

For a film made out of 5% w/w PDLLA/chloroform, which was immersed and kept in methanol for 1 day or longer, Van de Witte et al.<sup>11</sup> found that no structure was preserved. Comparison with our results

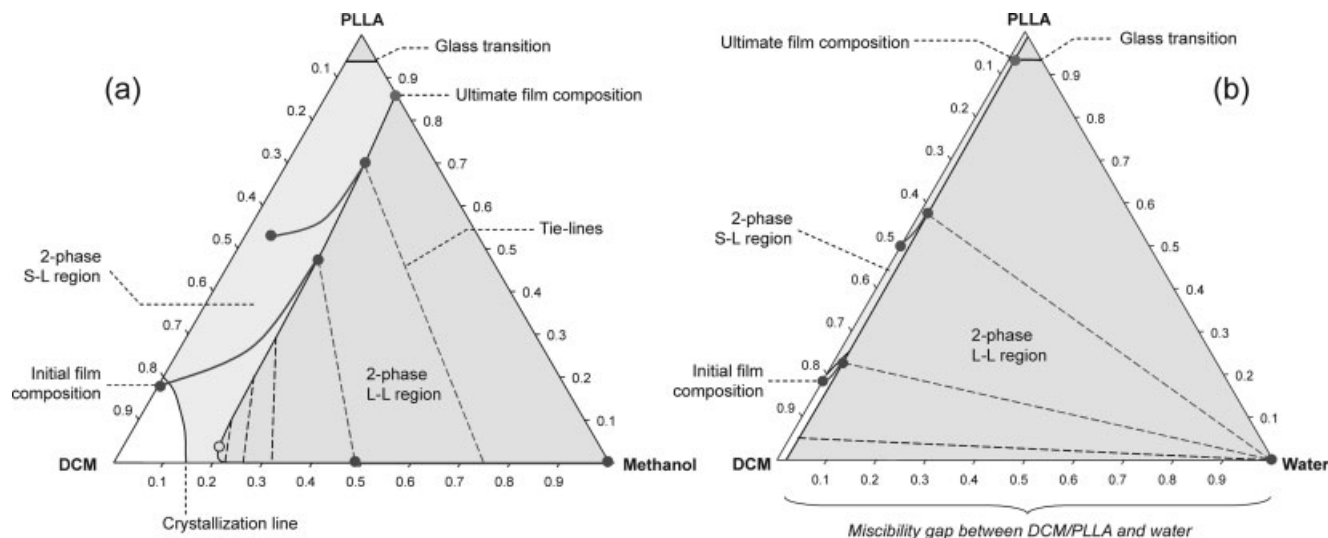


**Figure 6** Schematic phase diagrams of (a) PLLA–DCM–methanol and (b) PLLA–DCM–water systems. The crystallization line indicates fixation of the polymer-rich matrix by formation of crystals. The phase diagrams were calculated with the parameters as mentioned in Table I.

shows that increasing the polymer concentration reduces the time required for phase separation, and results in faster loss of structure.

#### PLLA: Nonsolvent effects

In contrast to PDLLA, PLLA is a rapidly crystallizing polymer.<sup>11,22,24</sup> Therefore, one may expect a strong influence of polymer crystallization, which will influence the morphology of the films as was reported in the literatures.<sup>6,9–11,24</sup> Films with polymer concentrations of 20% w/w PLLA/DCM were prepared using 100% methanol, 60 and 30% w/w methanol/water, and water as nonsolvents; the cross sections of the films are shown in Figure 5. The film prepared with methanol as nonsolvent consists of dense blobs surrounded by semicircular closed cells [Fig. 5(a)]. The top layer at the left of the image (the side in contact with the nonsolvent) has a very densely packed struc-

ture without pores. During film formation (see also Fig. 6 for the phase diagrams), the initial in-diffusion of nonsolvent is much smaller than the out-diffusion of the solvent.<sup>3</sup> Therefore, the polymer concentration in the top layer of the film rises quickly, which will bring the composition in this layer far inside the crystallization region of the phase diagram. Thus, the polymer will crystallize rapidly.

The out-diffusion of DCM from the sublayer to the nonsolvent bath is reduced significantly due to the additional mass transfer resistance created by the dense top layer. In spite of this, in time the concentration of DCM in the sublayer will be reduced, the solution will become more enriched with polymer, and the composition will approach the liquid–liquid miscibility gap. As soon as the miscibility gap is reached (after 16 s of immersion, see also Table II), liquid–liquid demixing by nucleation and growth of a polymer-lean phase will take place and a cellular structure is formed. The polymer concentration

**TABLE II**  
Light Transmission Results for PLLA–Dodecane–DCM Casting Solutions Immersed Into Different Methanol–Water Baths

PLLA (wt %)	Dodecane (wt %)	DCM (wt %)	Temperature (°C)	Nonsolvent bath (wt %)	$t_d$ (s)	$r_{max}$	$t_f$ (s)
20	0	80	Room	Methanol	15.9	0.076	82
20	5	75	Room	Methanol	6.7	0.016	92
20	5	75	Room	60% Methanol–40% Water	27.4	0.018	116
20	5	75	Room	Water	328.3	0.003	741
20	10	70	Room	Methanol	2.2	0.023	84
20	10	70	Room	60% Methanol–40% Water	18.1	0.026	69
20	10	70	Room	Water	140.1	0.006	358
20	10	70	62	Methanol	4.4	0.016	402
20	10	70	87	Methanol	9.4	0.015	766

$t_d$ , the delay time of demixing (s);  $r_{max}$ , the maximum demixing rate ( $1\text{ s}^{-1}$ );  $t_f$ , the time where demixing is complete (s). Standard deviations of parameters  $t_d$  and  $r_{max}$  are typically 10% or less.

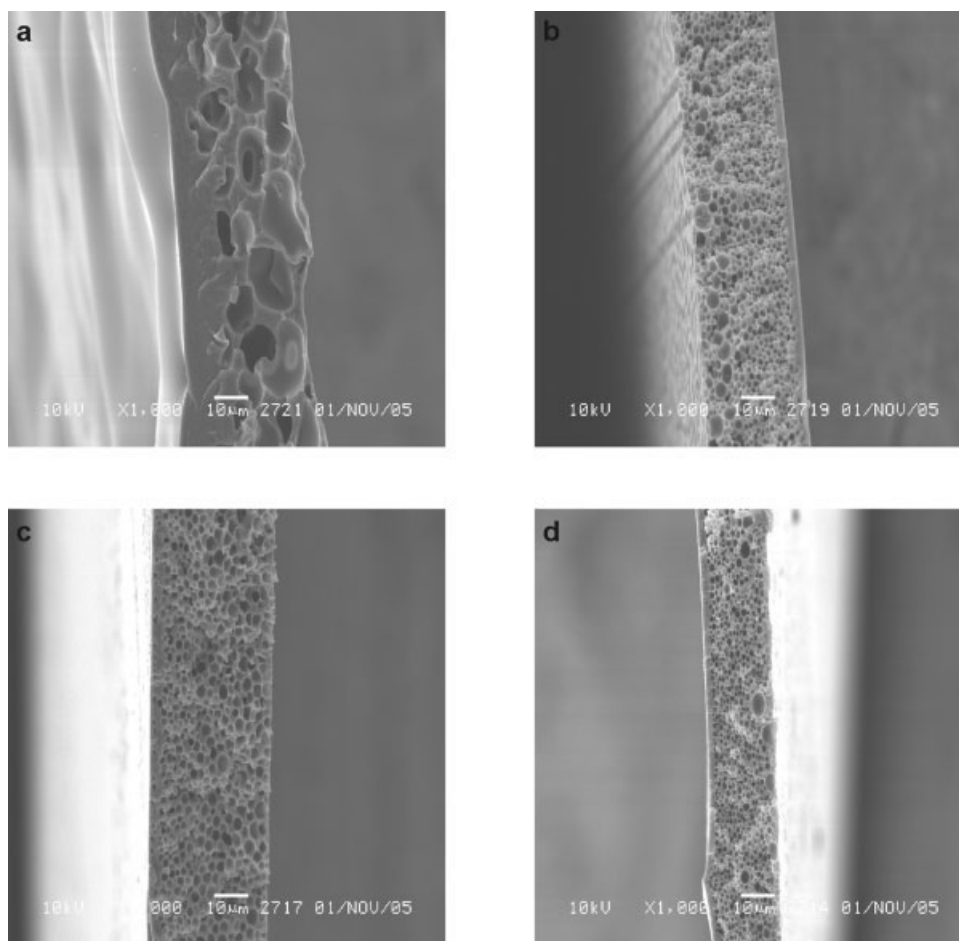


**Figure 7** SEM images of cross sections of films prepared from 20 : 10 : 70 w/w PDLLA : dodecane : DCM with different non-solvents: (a) methanol, (b) 60 : 40 w/w methanol : water, (c) 30 : 70 w/w methanol : water, (d) water; please note that the water film has been made out of film with a thinner initial thickness than the other films.

in the continuous phase will increase continuously until the solid–liquid demixing region is entered and crystallization of the polymer-rich phase occurs, which will form the dense blobs, and pore walls. It is expected that these solid blobs contain spherulites to such an extent that no distinction of the individual spherulites is possible anymore. This also becomes clear from the top view of the film [Fig. 5(b)], which shows a dense, nonporous film full of spherulites.

The occurrence of both phase separation processes (liquid–liquid demixing and crystallization) was observed for crystalline systems in general<sup>6,10</sup> and specifically for PLLA. For the PLLA–chloroform–methanol system, Van de Witte et al. demonstrated by DSC the presence of crystallites during the formation of PLLA membranes; further, they stated that at high PLLA concentration (>20% w/w) crystallization becomes the main demixing process, which affects to a large extent the morphology of the product.<sup>24</sup> Our results are in agreement with those of Van de Witte et al. for the same polymer concentrations.<sup>11</sup>

When water/methanol mixtures were used as non-solvent, the in-diffusion of methanol mixture and the

out-diffusion of DCM are slowed down, and the crystallization process has more time to proceed. Thus, we see that for higher water concentrations, the spherulites are more pronounced, larger and further apart [Figs. 5(c–f)]. Crystallization is expected to have taken place because of the slow exchange of the solvent and nonsolvent; the time available was long enough to initiate growth of the solid crystals. This case is schematically illustrated in the phase diagram (see Fig. 6), where the polymer concentration is slowly increased and after a relatively long time, the solid–liquid demixing region is entered and crystallization occurred in the film. The structure of the spherulites shows no signs of phase separation due to liquid–liquid demixing. It has been reported in literature that slow exchange rates between solvent and nonsolvent promote solid–liquid demixing over liquid–liquid demixing<sup>9,10</sup>; our findings are in line with this.

Even when only water was used in the coagulation bath, the cross section and the top view of the films were still similar [Figs. 5(e,f)]. The film shows a spherulitic, dense structure. In some places, the spherulites are fused at their point of contact or completely

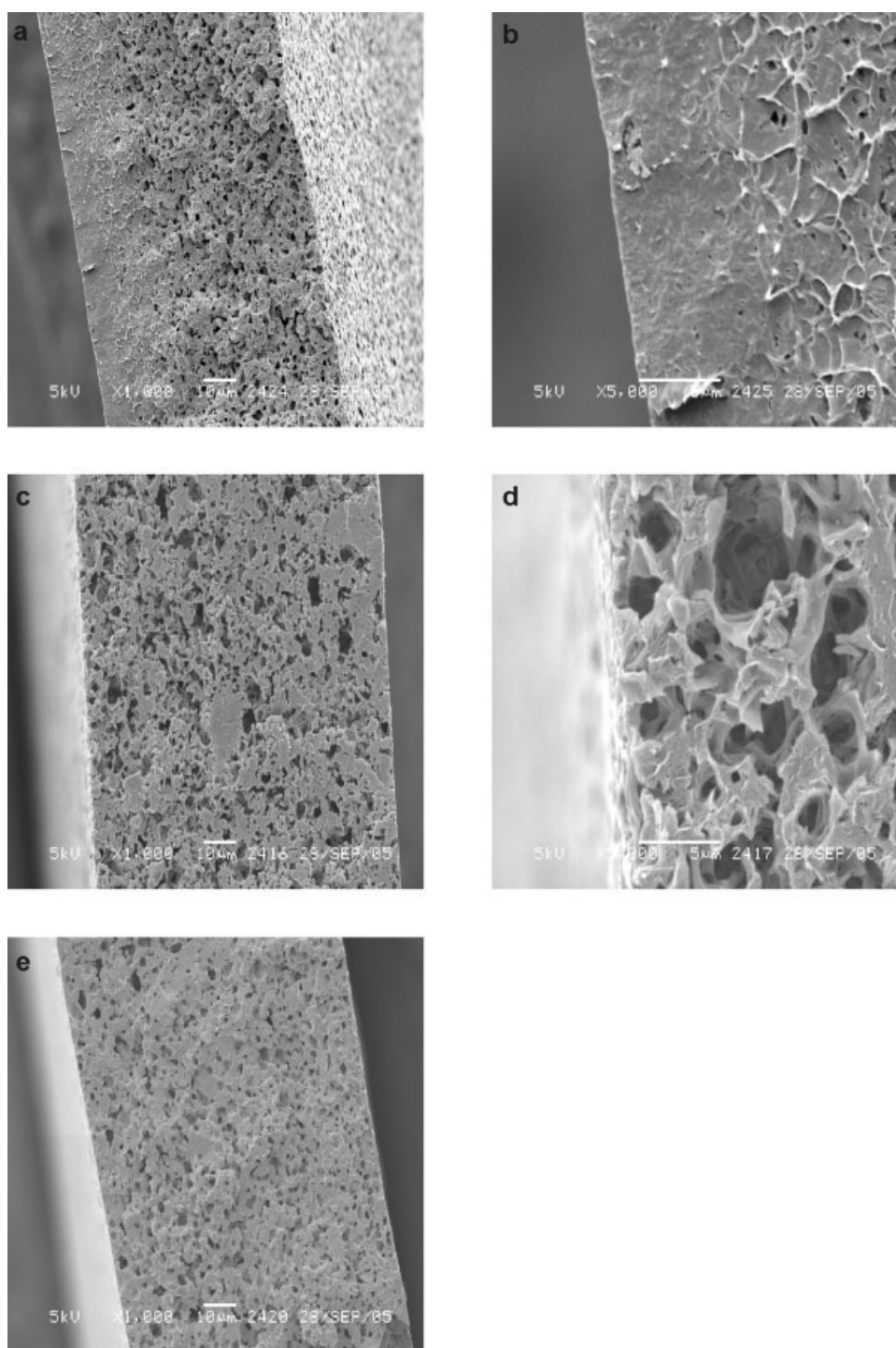


**Figure 8** SEM images of cross sections of films prepared from 20 : 5 : 75 w/w PLLA : dodecane:DCM with different nonsolvents: (a) methanol; (b) magnification of (a); (c) water; (d) magnifications of (c); (e) 60 : 40 w/w methanol : water.

blended together, forming a solid blob. Apparently, also in this case, phase separation has occurred by solid-liquid demixing, and perhaps some liquid-liquid demixing afterwards. The structure of films prepared with 60 and 30% w/w methanol/water [Figs. 5(c,d)] resemble the structure of the water film [Figs. 5(e,f)], as was also expected from the demixing times, results not shown.

#### **Addition of dodecane**

##### **Poly-DL-lactide**

The effect of an additive that is not miscible with either the polymer or with the nonsolvent applied in the coagulation bath was investigated by addition of 10% w/w dodecane to the casting solution. Compared to the situation without dodecane, the morphology of



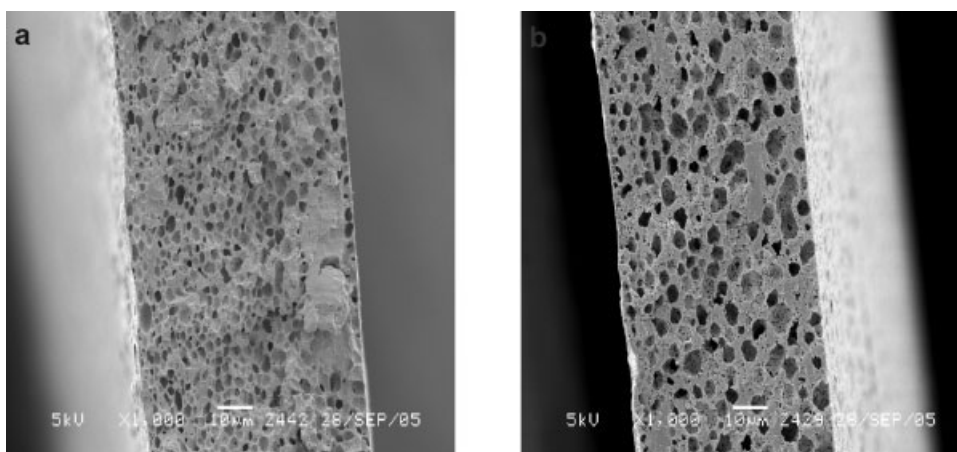


**Figure 9** SEM images of cross sections of films prepared from 20 : 10 : 70 w/w PLLA : dodecane : DCM with different non-solvents: (a) methanol, (b) water.

the films dramatically changed into a typical asymmetric morphology. The cross sections of these films show a dense skin layer with only little, small pores, and a porous sublayer with a fairly uniform closed cellular morphology [Figs. 7(a–d)]. In the film prepared from methanol, the dense skin is thicker and has no pores, while the porous sublayer contains big, irregular pores [Fig. 7(a)]. The explanation is the high exchange rate between methanol and solvent compared to the other nonsolvents. For methanol, the polymer concentration increased quickly at the film–bath interface resulting in a dense top layer. In the sublayer, the diffusion of solvent and nonsolvent slowed down because of the presence of the dense top layer, however, slowly but surely the dodecane concentration increased in the sublayer. As PDLLA is an amorphous polymer, liquid–liquid demixing was the predominant phase separation process, which resulted in the porous structure. As the methanol concentration inside the film slowly increased, the solubility of dodecane in the solution decreased accordingly, which ultimately resulted in the formation of droplets of dodecane; these droplets were the precursors of the cellular pores observed. It is remarkable that without dodecane the film collapses completely, while now some structure is preserved. The dodecane phase is trapped while the polymer solution surrounding it slowly becomes more viscous. As the out-diffusion of dodecane is extremely slow, the collapse becomes too slow. Thus, when we would have extended the residence time in the bath considerably, we would possibly have seen a slow reduction of the porosity as a function of the immersion time.

If the dodecane in PDLLA solution was replaced with an additive that is miscible with the nonsolvent as conventionally used, one would expect that the additive will diffuse out of the film, along with the solvent. The film would have collapsed into a dense structure, as without using an additive; no stabiliza-

tion of the structure could have taken place. The immiscibility of the additive ensures that it stays inside the film, forming the cellular pores. In the Appendix, the addition of dodecane and its effect on the phase behavior of the system is discussed in more detail for the interested reader.

#### Poly-L-lactide

To investigate the effects by crystallinity of the polymer, PLLA films with different dodecane concentrations were also prepared. In Figures 8 and 9, the SEM micrographs are shown for dodecane concentrations of 5 and 10% w/w, respectively. Figure 8 shows the cross sections of films prepared from 20 : 5 : 75 PLLA : dodecane : DCM. Compared to those without dodecane [e.g., Fig. 5(a)], the porosity of the films increased, the pores became larger and better connected, and consequently the structure was more open.

Demixing set in  $\sim 7$  s after immersion into the methanol bath (see Table II). The resulting film has an asymmetric structure consisting of a dense top layer and a porous sublayer, which consists of a bicontinuous network. The morphologies observed suggest a particular series of occurrences of liquid–liquid demixing and crystallization. We expect that initially, crystallization will set in, which depletes the surrounding solution of polymer, and which becomes more susceptible to liquid–liquid demixing, as they simultaneously become more concentrated in DCM and dodecane. This implies that the concentration of dodecane is expected to influence the structure as well.

When the same polymer solution was immersed in water, demixing occurred only very slowly ( $>6$  min) as indicated in Table II. The obtained film morphology differs strongly from the one formed with methanol [Figs. 8(c,d)]. The dense skin layer has disappeared and the structure consists of a few blobs embedded in

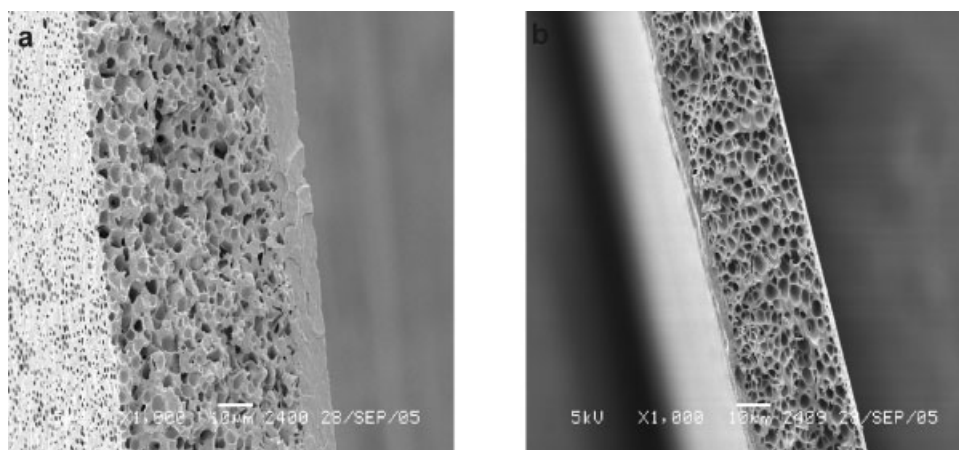


**Figure 10** SEM images of cross sections of films prepared from 20 : 10 : 70 w/w PLLA : dodecane : DCM solution heated at different temperatures and with methanol as nonsolvent: (a) 62°C, (b) 87°C.

a distorted, bicontinuous porous matrix. The pores were more open, interconnected, and irregular in shape and size. When a solution of 60% w/w methanol in water was used as nonsolvent, the delay time was in between those of methanol and water (Table II). The observed morphology was to some extent similar to the one obtained with water, but the structure is less porous and the pores are smaller, more closed, and less interconnected [Fig. 8(e)].

The effect of the dodecane concentration was investigated further, because we expected it to have an important role in the formation of the films. Figures 9(a, b) show the morphologies of films prepared with more dodecane (10% w/w) in the casting solution.

The porosity and the size of the pores increase by increasing the dodecane concentration. In case of methanol as nonsolvent [Fig. 9(a)], pores can be observed in the top layer, and the film contains some dense areas embedded in a more regular cellular structure with bigger pores, compared to the film prepared with 5% dodecane [Fig. 8(a)]. With water, the film has a more open morphology with high interconnectivity and big spherical pores as shown in Figure 9(b). This could be related to an increased probability of coalescence of dodecane droplets due to the long diffusion times, resulting in bigger pores. Similar effects as described for methanol occurred for the film prepared from 60% methanol (result not shown).

From the light transmission results, it is clear that increasing the amount of dodecane in the casting solution decreases the delay time for demixing (Table II). As the solution is less stable with the nonsolvent dodecane present (i.e., the starting composition is closer to the border of the demixing gap in the phase diagram), phase separation will start at an earlier stage, at which droplets of a dodecane-rich phase will be formed [see Fig. 9(a)]. The remaining PLA-DCM solution will then demix according to a normal (delay of) demixing regime with methanol (Fig. 6), which will

result in smaller pores in the matrix surrounding the larger pores formed by the dodecane. In the Appendix, the addition of dodecane and its effect on the phase behavior of the system is discussed in more detail for the interested reader.

#### Effect of temperature

Casting solutions with 10% w/w dodecane were heated up and after some time cooled down to room temperature, before immersion in the nonsolvent bath. When the film was produced from a solution that was incubated at 87°C, crystallization set in after longer delay time (Table II) and the skin layer was thinner than with a solution that was incubated at 62°C. Besides that, the porous sublayer contained a closed cellular structure [see Figs. 10(a,b)]. This indicates that the crystallization process depends on nuclei already present in the casting solution. Heating the solution before casting, results in melting of many of the nuclei. This suppresses the crystallization process. Therefore, liquid–liquid demixing is relatively faster in these films. Therewith, a cellular morphology was obtained and the crystallization-associated structures such as the observed solid blobs [compare with Fig. 9(a)] were not present. We now see structures that are similar to the ones observed with the amorphous PDLLA; the structures are now fixated after some time by crystallization. This stresses the importance of control of crystallinity of the polymer in the production of structures with a desired morphology, especially in combination with the use of another nonsolvent like dodecane in the polymer solution.

In general, it is clear that the use of dodecane as a nonsoluble additive leads to new opportunities to influence porosity in polymeric films and structures. In combination with the choice of solvent, nonsolvent, and other process conditions, this may open a new road to the design of highly porous structures.

## CONCLUSIONS

Films formed from solutions of amorphous PDLLA show a dense structure; any porous structure formed during demixing collapses, since fixation by crystallization or vitrification cannot take place. With crystalline, PLLA-specific morphologies are obtained. With methanol as nonsolvent, a typical asymmetric structure formed by crystallization and (delayed) liquid–liquid demixing was found. With water as nonsolvent, which is hardly miscible with the solvent, the demixing rate was much lower. Liquid–liquid demixing was suppressed and crystallization dominated the formed, symmetric structure.

Next, the influence of an additive, dodecane, which is immiscible with the nonsolvent was investigated. Addition of dodecane speeds up demixing and increases the porosity of the films. Remarkably, for PDLLA, the film does not collapse, as a result of the presence of dodecane droplets, and retains a closed-cell structure. For PLLA films, addition of dodecane made the structure more open and better interconnected. This effect seems stronger than that with miscible additives.

The differences in structure between PLLA and PDLLA became smaller when PLLA solution was given a heat pretreatment before casting to remove nuclei for crystallization. Liquid–liquid demixing became the dominant mechanism, and crystallization served to stabilize the obtained structure.

We thank our project partners from Philips Research in Eindhoven, Erasmus Medical Centre in Rotterdam, and the Physics of Fluids group from Twente University in Enschede for fruitful discussions. Special thanks go to Marcel Bohmer from Philips for proofreading our manuscript. The authors would further like to thank ing. H.A. Teunis, Membrane Technology Group, University of Twente for his help in the SEM analysis, which is very much appreciated, and Dr. ir. R.G.H. Lammertink, Membrane Technology Group, University of Twente for making the light transmittance setup available.

## APPENDIX

Based on the results presented previously, one can conclude that the addition of dodecane to the casting solution has a big influence on the film structure. The presence of dodecane in the polymer solution has lowered the solvent quality of DCM, which will influence the phase separation mechanism. The presence of dodecane in the casting solution has brought the demixing gap much closer to the initial polymer cast composition. This is consistent with the light transmission results. Increasing the dodecane concentration from 0 to 5% reduces the delay time from 16 to 7 s. Upon further increase of the dodecane concentration, the delay

time is reduced further until we have almost instantaneous demixing at 10% dodecane (Table II).

A possible but very unlikely interpretation for the system is that the mixture of DCM and dodecane might actually function as a cosolvent for PLA. If the cosolvency holds, the phase diagram can have two demixing regions with two binodal curves sandwiching a miscibility region as described by Cheng and Shaw for the system of poly(methyl methacrylate) in water–2-propanol cosolvent mixtures,<sup>25</sup> and by Tao and Young using poly(*N*-isopropylacrylamide) in water–methanol cononsolvent mixtures.<sup>26</sup> In such a case, the demixing region in the phase diagram will increase in size, which will most probably facilitate phase separation. However, it should be kept in mind that dodecane is a poor solvent for PLA and it is not expected that dodecane/DCM mixtures can act as a cosolvent.

The incorporation of dodecane to the casting solution makes the system more complex as it has become a quaternary system. The principle is however the same as for the ternary one. Contacting the polymer solution with nonsolvent will cause out-diffusion of solvent and a smaller in-diffusion of nonsolvent, and consequently demixing will take place.

Figure 1 shows the folded-down quaternary phase diagrams—these are the ternary limiting systems of the full (three-dimensional) diagrams. Please note that only binodals and tie-lines are shown and not spinodals. Earlier research has shown that demixing by immersion leads to metastable demixing and not spinodal decomposition—thus the binodals are most relevant for our purpose.<sup>27</sup> The PDLLA–DCM–methanol–dodecane system (a) shows three two-phase regions, indicating an equilibrium between a PLA-concentrated and a PLA-diluted phase. For truly quaternary solutions, these two-phase regions lead to a three-phase region, which is inside the quaternary phase diagram, and not visible in the limiting ternary diagrams. This can be illustrated by assuming a quaternary solution containing equal amounts of all four components. This solution will decompose into a PLA-rich and a PLA-poor phase. This PLA-poor phase would contain roughly equal amounts of the three low-molecular weight components. This phase is not stable (see limiting ternary DCM–dodecane–methanol diagram) and will itself decompose into a phase rich in methanol and a phase rich in dodecane. Thus, a three-phase region is present inside the quaternary phase diagram, as a result of the three two-phase regions in the limiting ternary diagrams. This same three-phase region is evident in the limiting ternary system methanol–dodecane–PDLLA: most of the phase diagram is occupied by a three-phase region, indicating decomposition of the compositions enclosed by the region, into a methanol phase, a dodecane phase, and a PDLLA-rich phase. Around this three-phase region, two two-phase regions are visible.

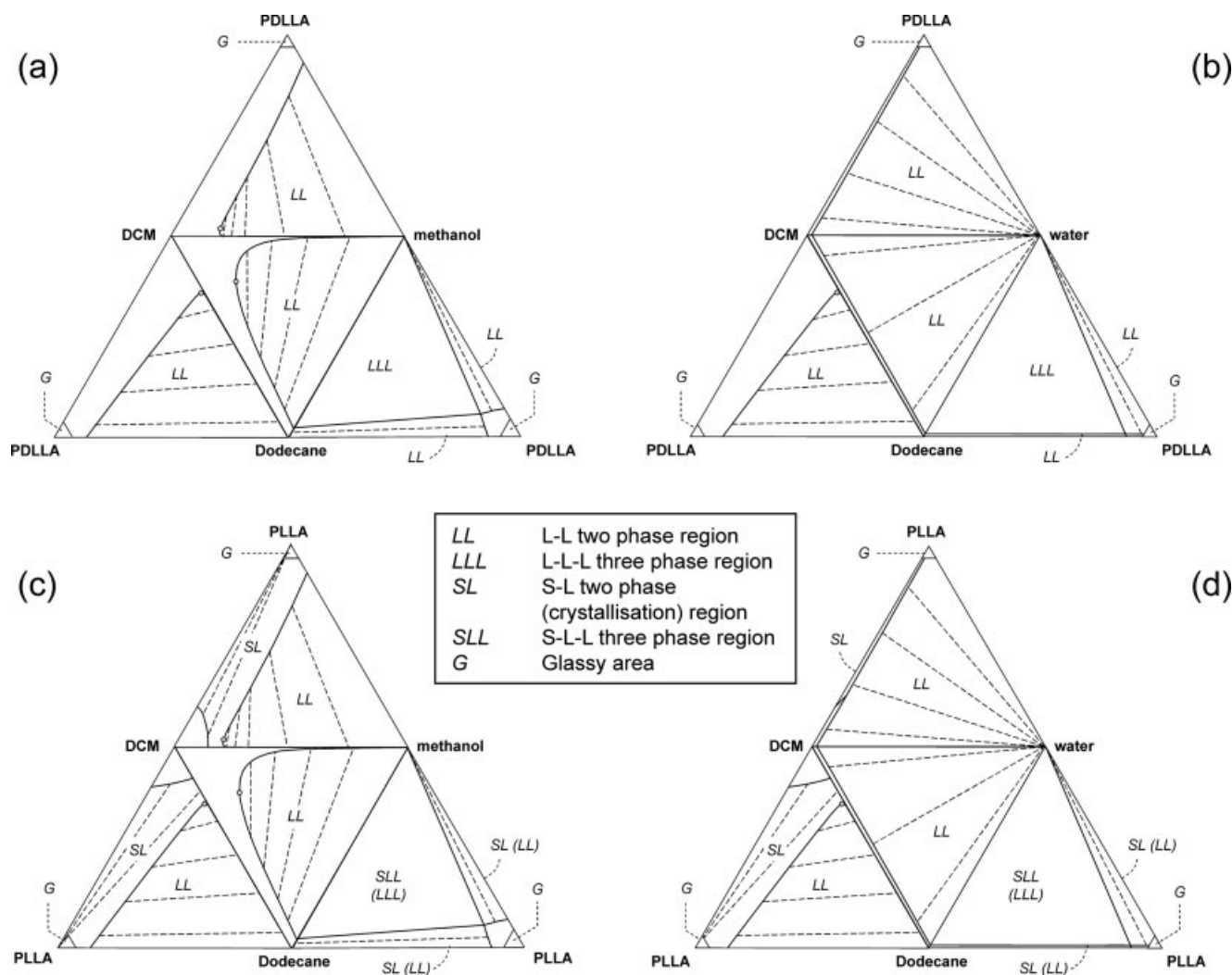


**Figure A1** Full quaternary (folded-out) phase diagrams for (a) PDLLA–DCM–methanol–dodecane, (b) PDLLA–DCM–water–dodecane, (c) PLLA–DCM–methanol–dodecane, and (d) PLLA–DCM–water–dodecane. The phase diagrams were calculated with the parameters as mentioned in Table I.

The system with water instead of methanol (b) shows a somewhat different phase diagram due to the relative immiscibility of water with the other components. Solutions of PDLLA with DCM are basically immiscible with water, leading to a large two-phase region in that limiting ternary diagram. Since dodecane is immiscible with water as well, a similar demixing gap is visible in the ternary system DCM–dodecane–water. The three two-phase regions in the systems PDLLA–DCM–water, DCM–dodecane–water and DCM, dodecane–PLA, once more lead to a three-phase region inside the quaternary phase diagram, which is evident in the limiting diagram for water–dodecane–PDLLA.

The systems with PLLA (c and d) show the same liquid–liquid demixing behavior as with PDLLA, but in addition show regions exhibiting demixing between a crystalline PLLA phase and a liquid (PLLA-poor) phase. They are visible in the limiting

phase diagrams PLLA–DCM–methanol, PLLA–DCM–dodecane, PLLA–DCM–water, and PLLA–DCM–dodecane: once more, these regions extend into the volume of the quaternary phase diagrams. Even though in the ternary systems PLLA–dodecane–methanol and PLLA–dodecane–water no crystallization areas are visible, one should bear in mind that the stable PLLA-rich phases in the lower right corner of the diagram will be strongly crystallized. Below the liquid–liquid demixing gaps (two-phase and three-phase) a crystallization curve is present, which means that even though thermodynamically speaking, the three-phase region is a liquid–liquid–liquid region, the actual three-phase equilibrium will be of type liquid–liquid–solid (water/methanol phase, dodecane phase, and crystallized PLLA phase).

The phase diagrams show that PLLA systems have a strong tendency to crystallize, even before liquid–liquid demixing. However, crystallization is generally

a slow process. Since liquid–liquid demixing is usually a fast process (except when the nonsolvent diffuses in very slowly), liquid–liquid demixing can still take place before crystallization can take place.

## References

1. Van de Witte, P.; Dijkstra, P. J.; Van den Berg, J. W. A.; Feijen, J. *J Membr Sci* 1996, 117, 1.
2. Tanaka, T.; Lloyd, D. R. *J Membr Sci* 2004, 238, 65.
3. Reuvers, A. J.; Smolders, C. A. *J Membr Sci* 1987, 34, 67.
4. Wienk, I. M.; Boom, R. M.; Beerlage, M. A. M.; Bulte, A. M. W.; Smolders, C. A.; Strathmann, H. *J Membr Sci* 1996, 113, 361.
5. Young, T. H.; Cheng, L. P.; Lin, D. J.; Fane, L.; Chuang, W. Y. *Polymer* 1999, 40, 5315.
6. Bulte, A. M. W.; Mulder, M. H. V.; Smolders, C. A.; Strathmann, H. *J Membr Sci* 1996, 121, 51.
7. Cheng, L. P.; Young, T. H.; You, W. M. *J Membr Sci* 1998, 145, 77.
8. Lin, D. J.; Chang, C. L.; Chen, T. C.; Cheng, L. P. *Desalination* 2002, 145, 25.
9. Van de Witte, P.; Esselbrugge, H.; Dijkstra, P. J.; Van den Berg, J. W. A.; Feijen, J. *J Polym Sci Part B: Polym Phys* 1996, 34, 2569.
10. Bulte, A. M. W.; Folkers, B.; Mulder, M. H. V.; Smolders, C. A. *J Appl Polym Sci* 1993, 50, 13.
11. Van de Witte, P.; Esselbrugge, H.; Dijkstra, P. J.; Van den Berg, J. W. A.; Feijen, J. *J Membr Sci* 1996, 113, 223.
12. Zoppi, R. A.; Contant, S.; Duek, E. A. R.; Marques, F. R.; Wada, M. L. F.; Nunes, S. P. *Polymer* 1999, 40, 3275.
13. Yeow, M. L.; Liu, Y. T.; Li, K. *J Appl Polym Sci* 2004, 92, 1782.
14. Cheng, L. P. *Macromolecules* 1999, 32, 6668.
15. Cheng, L. P.; Huang, Y. S.; Young, T. H. *Eur Polym J* 2003, 39, 601.
16. Chuang, W. Y.; Young, T. H.; Chiu, W. Y.; Lin, C. Y. *Polymer* 2000, 41, 5633.
17. Chuang, W. Y.; Young, T. H.; Chiu, W. Y. *J Membr Sci* 2000, 172, 241.
18. Van de Witte, P.; Esselbrugge, H.; Peters, A. M. P.; Dijkstra, P. J.; Feijen, J.; Groenewegen, R. J. J.; Smid, J.; Olijslager, J.; Schakenraad, J. M.; Eenink, M. J. D.; Sam, A. P. *J Controlled Release* 1993, 24, 61.
19. Madaeni, S. S.; Rahimpour, A.; Barzin, J. *Iranian Polym J (English Edition)* 2005, 14, 421.
20. Zhao, J.; Yuan, X.; Cui, Y.; Ge, Q.; Yao, K. *J Appl Polym Sci* 2004, 91, 1676.
21. Pego, A. P.; Siebum, B.; Van Luyn, M. J. A.; Gallego y Van Seijen, X. J.; Poot, A. A.; Grijpma, D. W.; Feijen, J. *Tissue Eng* 2003, 9, 981.
22. Tsuji, H. *Macromolecules* 1992, 25, 5719.
23. Urayama, H.; Kanamori, T.; Kimura, Y. *Macromol Mater Eng* 2002, 287, 116.
24. Van de Witte, P.; Boorsma, A.; Esselbrugge, H.; Dijkstra, P. J.; Van den Berg, J. W. A.; Feijen, J. *Macromolecules* 1996, 29, 212.
25. Cheng, L. P.; Shaw, H. Y. *J Polym Sci Part B: Polym Phys* 2000, 38, 747.
26. Tao, C. T.; Young, T. H. *Polymer* 2005, 46, 10077.
27. Radovanovic, P.; Thiel, S. W.; Hwang, S. T. *J Membr Sci* 1992, 65, 213.